J. Cent. South Univ. (2016) 23: 2146−2155
DOI: 10.1007/s11771-016-3271-1

Springer

Application of artificial neural network to predict Vickers microhardness of AA6061 friction stir welded sheets

Vahid Moosabeiki Dehabadi[1], Saeede Ghorbanpour[1], Ghasem Azimi[2]

1. Department of Mechanical Engineering, K. N. Toosi University of Technology, Tehran, Iran;
2. Educational Workshop Center, Isfahan University of Technology, Isfahan, Iran

Abstract: The application of friction stir welding (FSW) is growing owing to the omission of difficulties in traditional welding processes. In the current investigation, artificial neural network (ANN) technique was employed to predict the microhardness of AA6061 friction stir welded plates. Specimens were welded employing triangular and tapered cylindrical pins. The effects of thread and conical shoulder of each pin profile on the microhardness of welded zone were studied using tow ANNs through the different distances from weld centerline. It is observed that using conical shoulder tools enhances the quality of welded area. Besides, in both pin profiles threaded pins and conical shoulders increase yield strength and ultimate tensile strength. Mean absolute percentage error (MAPE) for train and test data sets did not exceed 5.4% and 7.48%, respectively. Considering the accurate results and acceptable errors in the models' responses, the ANN method can be used to economize material and time.

Key words: friction stir welding; artificial neural network; aluminum 6061 alloy; Vickers microhardness

1 Introduction

Aluminum and aluminum alloys have been used widely due to the light weight and high specific strength in comparison with other metals [1−2]. Among the aluminum alloys, AA6061 is more prevalent in aerospace and automobile industries due to the high specific strength and corrosion resistance [1−3]. The high-tech applications of aluminum and its alloys specify the need of methods for welding these metals [4]. Conventional methods of welding, like fusion welding, have restrictions for a large number of metallic alloys which are difficult-to-weld or non-weldable and may result in crack and porosity in welded aluminum alloy plates [5−7].

Therefore, other novel methods like friction stir welding are developing as the solid state, hot shear joining process to overcome the aforementioned difficulties [6−9]. FSW in aluminum alloys reduces the deformation and residual stresses and enhances the mechanical properties of weld in comparison with traditional methods [10−11]. In the FSW, a non-consumable rotating tool moves along the surfaces of the two plates which are firmed. Friction between the shoulder of the tool and plates makes a large amount of heat which causes severe plastic deformation in the plates, and the movement of the tool in the welding direction makes a flow of metal. This method of welding is appropriate for metals which cannot be welded by traditional methods particularly aluminum alloys [7, 12−13].

Various modeling methods including artificial neural network (ANN) methods have been employed in order to develop the applications of FSW and reduce the costs of experiments. ANNs are mathematical methods which are capable to model the physical processes and predict the final properties. In Refs. [5, 12, 14−17], ANNs were used to predict and determine the mechanical properties in friction stir welding. OKUYUCU et al [5] utilized a single hidden layer feed-forward ANN to study the relationship between rotational and weld speed, and mechanical properties in Al plates. The features which they considered as outputs comprise of tensile and yield strength, hardness of HAZ and weld metal, and elongation. BUFFA et al [12] used two ANNs to predict the microhardness and the microstructure of Ti-6Al-4V titanium alloy which was welded by FSW method. SHOJAEEFARD et al [14] developed an artificial neural network to model the FSW parameters in Aluminum alloys welding. In their work, the effect of weld and rotational speed on the mechanical properties such as hardness and ultimate tensile strength was evaluated. SHOJAEEFARD et al [15] investigated the influence of weld and rotational speed on peak temperature, HAZ width, and welding force in AA5083

Received date: 2015−07−22; **Accepted date:** 2015−12−25
Corresponding author: Vahid Moosabeiki Dehabadi, Master; Tel: +98−21−88888800; Cell: +98−913−3599995; E-mail: v.moosabeiki@sina.kntu.ac.ir

aluminum alloy. GHETIYA et al [16] designed a back propagation neural network to predict the mechanical properties of friction stir welded aluminum alloy. Tool shoulder diameter, welding and rotational speed and axial force were the parameters that their effect was investigated on the tensile strength of the weld.

Although the material flows and consequently, the mechanical properties of weld in FSW are highly affected by tool geometry [3, 5, 13, 18], it was discussed in a few literature [16]. Current study aims to investigate the effect of tool pin profile including tool tilt angle and thread of pin on the microhardness of weld and plates using ANN method. Preparing the required data for training the neural networks as well as determining the effects of aforementioned parameters on the final microhardness of welded plates, AA6061 aluminum alloys were welded and samples were produced using two kinds of pin profiles including triangle and tapered cylindrical shaped pins. The obtained data were conducted to establish neural networks which were able to predict the Vickers microhardness of friction stir processed plates.

2 Materials and methods

2.1 Samples preparation

AA6061 aluminum alloy sheets with the dimensions of 130 mm×100 mm×6 mm were welded using various tool pin profiles. The chemical composition of the sheets is given in the Table 1.

Table 1 Chemical composition of AA6061 aluminum alloy sheets (mass fraction, %)

B	Zn	Cr	Mg	Mn	Fe	Cu	Si	Al
0.06	0.1	0.03	0.35	6.03	0.5	0.1	0.3	Remained

The tool profile is one of the most vital parameters and affects the weld zone properties. Basically, it comprises of a shoulder and a pin as shown in Fig. 1. Tools which were used in the current study were made of non-consumable high carbon steel (H13), and the physical features of the utilized tool are summarized in Table 2.

In order to evaluate the effects of thread and tool tilt angle on the microhardness of the welded aluminum alloy sheets, two various shapes of pin including triangle and tapered cylindrical with three different geometries of tools for each shape were manufactured and considered in the present research. Among three manufactured pins for each profile, one pin was threaded and the shoulder had an 8° tilt angle, while, two remaining threadless pins had flat and inclination cavity shoulder, which are illustrated in Figs. 2 and 3. In order to fabricate targeted

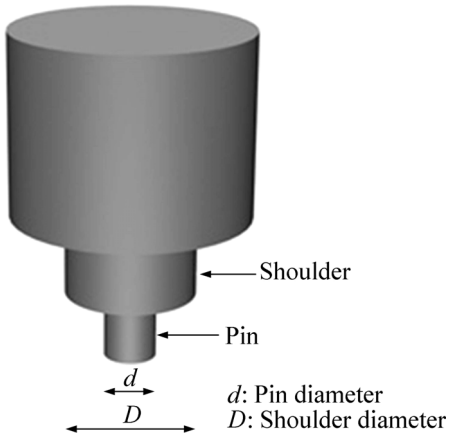

Fig. 1 Initial parts of tool in friction stir welding [12, 16]

Table 2 Features of FSW tool in this work

Tool material	Initial hardness (HRC)	Hardness during welding (HRC)	Pin length/mm
H13 Steel	60	56	5.5

tools, after obtaining adequate height and diameter, tools were heat treated followed by grinding to achieve the sufficient hardness. Furthermore, since the pin is more involved in welding compared with the body, its hardness had been enhanced by 15HRC in comparison with the body (60HRC in the tip versus 45HRC in the body of pin).

Over the present investigation, friction stir welding was processed in the room temperature and without any filler, gas and flux. Having reduction in contact between tools' shoulder and sheets, the angle between tools and sheets was chosen 87° instead of vertical position. Foresaid position increased the weld speed hence the axial force decreased. The rotational and traverse speeds were adjusted and considered constant at 1000 r/min and 28 mm/min, respectively. After welding process, the appearance, microstructure and microhardness of the welded samples were investigated. Using Macro-Etch technique on the AA6061 aluminum alloy sheets, the microstructure of welded samples were studied and any probable defects were detected. First of all, samples were polished using abrasive papers (numbers 80, 320, 600, and 1200) which were coated with tungsten carbide. Following, samples were etched using the Keller's reagent, and the optimum time of etching was determined to be 5 s considering the results of experimental tests. In addition, to evaluate the tensile strength, yield strength, and fracture type, tensile tests were used and friction stir welded sheets were prepared based on the ASTM-E08M standard as test samples. Tensile tests were carried out using Hounsfield testing machine which was able to apply a maximum load of 5000 kg.

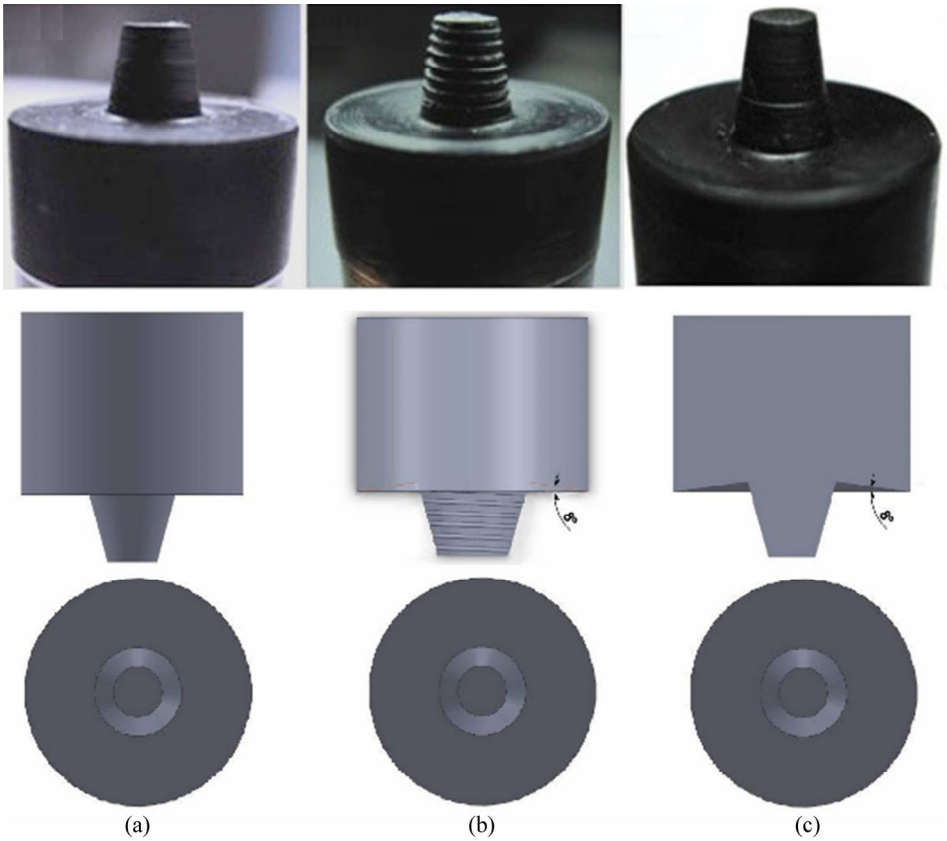

Fig. 2 Various profiles of tapered cylindrical tool: (a) Threadless pin, flat shoulder; (b) Threaded pin, conical shoulder; (c) Threadless pin, conical shoulder

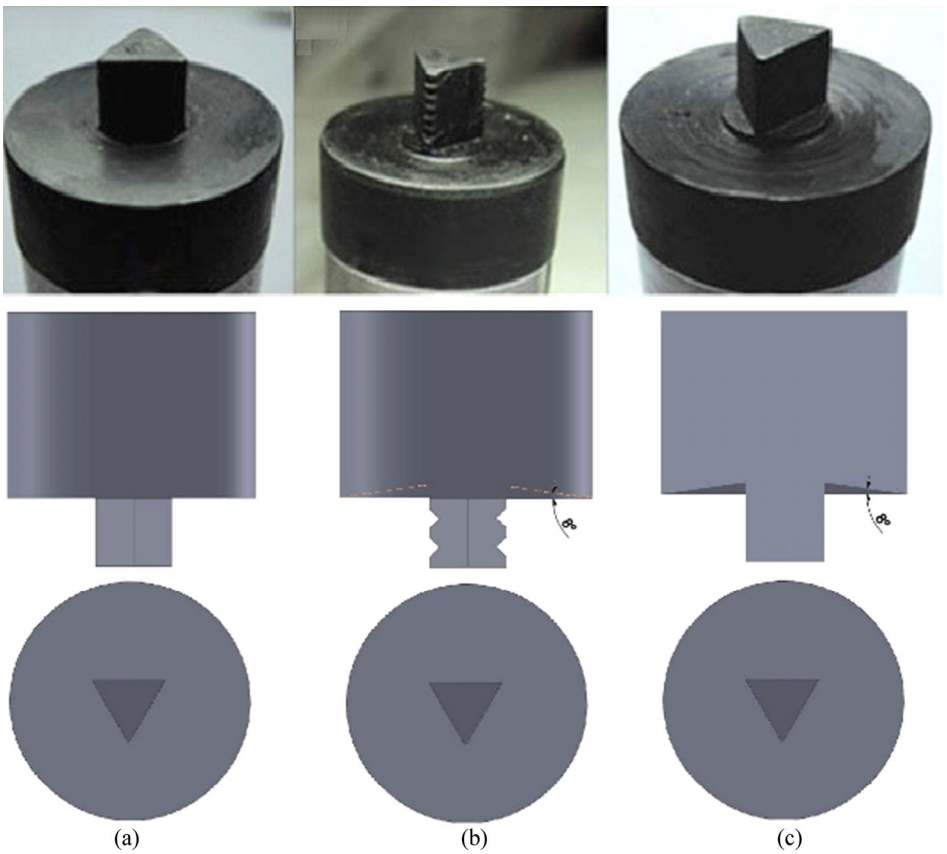

Fig. 3 Various profiles of triangle tool: (a) Threadless pin, flat shoulder; (b) Threaded pin, conical shoulder; (c) Threadless pin, conical shoulder

Vickers microhardness tests were employed to measure the hardness of welded samples. Therefore, the amount of load in tests was considered to be 98.07 mN and duration of load applied was 10 s (HV 0.01). Through the microhardness measurement process, the average of three spots was considered an associated microhardness result and utilized in the artificial neural network analyses.

2.2 Artificial neural network

Artificial neural network models are able to learn from examples and recognize the patterns between input and output data sets, and generalize the results for variable cases [19−20]. In the present investigation, MATLAB R2014a was utilized to model the effect of tool geometry and thread on the Vickers microhardness in various distances from welding centerline. Two applicable kinds of pin profiles were considered and some experimental tests were carried out in order to gather data. 51 and 48 data sets were appropriate to be used in the modeling for triangle and tapered cylindrical shaped pin respectively. Through the proposed analyses, tool tilt angle, thread, and distance from welding centerline considered input parameters, Vickers microhardness of welded plates was chosen as the output. An appropriate neural network was allocated to each pin profile (triangle and tapered cylindrical shaped) and each one had three inputs versus one output. Moreover, the data related to spots from one side of centerline were considered for the values of microhardness in two sides of weld center were approximately symmetric.

In the training procedure, four sets of the acquired experimental data for each pin profile were selected randomly, in order to test the trained network (named test data sets). The remaining sets were used in the training procedure including train, validation and test steps. Each ANN estimated the Vickers microhardness using the experimental data sets and initial weights and biases. Subsequently, the predicted answers of the network were compared with the actual results, and errors as well as mean absolute percentage error (MAPE), and mean absolute error (MAE) were calculated using Eqs. (1), (2) and (3), respectively. Over the training procedure, the weights were adjusted, and ANN continued its hardness predictions until it reached reliable errors. Mean squared Error (MSE) in validation step which is described by Eq. (4) is another important factor to terminate the training process.

$$E=\frac{A_i-Y_i}{A_i}\times 100 \tag{1}$$

$$\mathrm{MAPE}=\frac{1}{N}\sum_{i=1}^{N}\left(\frac{|A_i-Y_i|}{A_i}\right)\times 100 \tag{2}$$

$$\mathrm{MAE}=\frac{1}{N}\sum_{i=1}^{N}|Y_i-A_i| \tag{3}$$

$$\mathrm{MSE}=\frac{1}{N}\sum_{i=1}^{N}(A_i-Y_i)^2 \tag{4}$$

where A_i and Y_i referred to experimental and predicted Vickers microhardness of the data set number i respectively; and N indicated the number of all utilized data in the training process. The aforesaid procedure was done for each of neural networks separately.

A neural network with appropriate architecture performs properly and the results could be reliable. Hence, adequate hidden layers containing proper neurons had to assign to the network. Consequently, for each pin profile, neural networks including one, two and three hidden layers were examined along with various numbers of neurons between two and ten in the hidden layers. Coefficient of determination, MSE and MAPE were chosen as vital criteria to evaluate the suitable networks. Other factors which had significant influences on the accuracy of answers were learning and transfer functions. To assign the most appropriate functions to the ANNs, MSE, MAPE, and R^2 were appraised when learning functions chose Learngd and Learngdm. Besides, different transfer functions including tansig, purelin and logsig were used between input and hidden layers, as well as hidden and output layers through the training procedure. Tables 3 and 4 summarize some results for ANNs were trained using various combinations of hidden layers and neurons; and different transfer functions were for triangle and tapered cylindrical pins, respectively. Comparing the major factors for ANNs in Tables 3 and 4 indicates that the ANNs containing one and two hidden layers had the best performance for triangle and tapered cylindrical tools, respectively. Therefore, 3-8-1 and 3-7-3-1 structures, which are shown in Fig. 4, were the best architectures for predicting microhardness of AA6061 welded plates using triangle and tapered cylindrical pins.

3 Results and discussion

In general, the weld appearance in friction stir welding has a higher quality compared with the traditional methods of welding. In samples which were welded using threaded pins, the weld quality was significantly better than the others.

In other words, generating heat, which comes from the friction between the pin and sheets, and traversing force in threaded tools are higher than unthreaded ones [21−22], which can lead to a better weld quality. In addition, samples which were welded using tools with concave shoulders, showed better appearance in comparison with flat shoulder tools as materials are

Table 3 Results of some networks trained by various transfer functions, learning functions and structures for triangle pin profile

No.	Structure	Transfer function	Validation MSE	MAPE/%	R^2
1	3-8-1	Tansig-tansig	3.4972	5.5616	0.775
2	3-4-7-1	Logsig-tansig	7.012	6.3943	0.7268
3	3-5-6-1	Tansig-tansig	5.0315	5.7399	0.7545
4	3-6-4-1	Tansig-tansig	4.2268	5.522	0.7508
5	3-5-6-2-1	Tansig-logsig	4.8921	6.3865	0.681

Table 4 Results of some networks trained by various transfer functions, learning functions and structures for tapered cylindrical pin profile

No.	Structure	Transfer function	Validation MSE	MAPE/%	R^2
1	3-6-1	Tansig-tansig	13.31	6.642	0.7268
2	3-7-3-1	Tansig-tansig	9.437	4.5464	0.8479
3	3-7-5-1	Tansig-tansig	5.4302	6.5267	0.7662
4	3-4-5-1	Logsig-tansig	8.8748	6.3262	0.8179
5	3-3-6-2-1	Tansig-logsig	9.8756	6.76	0.6908
6	3-6-5-2-1	Tansig-tansig	12.3	5.9338	0.7907

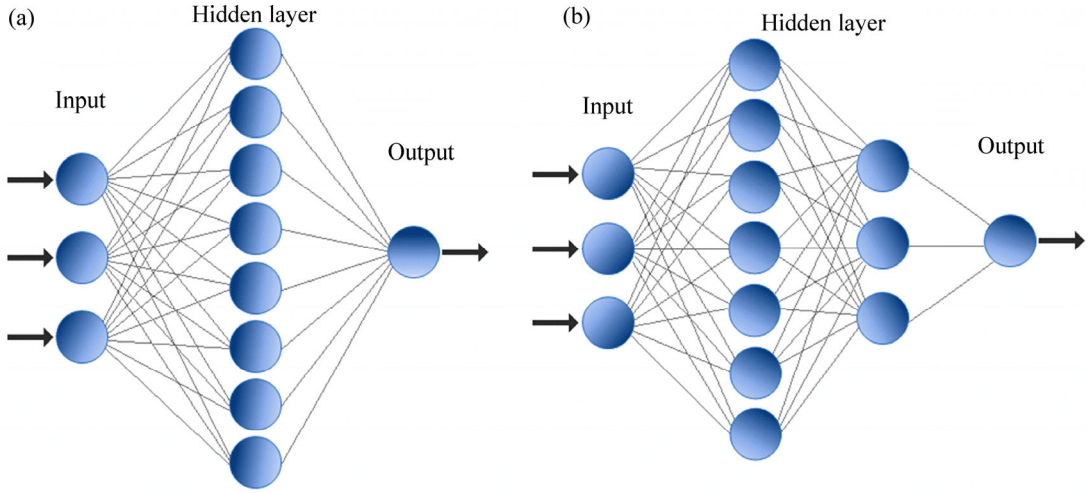

Fig. 4 Schematic of neural networks in this work for predicting Vickers microhardness in triangle (a) and tapered cylindrical (b) pin profile tools

located under the curve in conical shoulder and held to the vacancies near the shoulder which results in a better quality in the welded sheets [23−25].

Figure 5 shows the friction stir welded area of two samples after Macro-Etch process [6]. Plastic deformation had not occurred in the heat affected zone (HAZ) grains; however, the properties in HAZ had been changed due to the high amount of temperature. The properties in the HAZ area which may change comprising of strength, toughness, elongation, and corrosion resistance while the grain size and chemical composition have been remained as the same. Heating in the HAZ for aluminum alloys causes recovery of cold work and coarsening of precipitates which consequently lead to alteration in properties [26].

Thermo-mechanically affected zone (TMAZ) area includes all the metal which experienced plastic deformation. In this zone, sheets had been heated to high temperature and due to the high values of forces, plastic deformation has been observed in initial grains. TMAZ can be divided to non-recrystallization TMAZ and recrystallization TMAZ or nugget. for aluminum alloys; non-recrystallization TMAZ is more important since the reduction of microhardness values and corrosion resistance occur in this zone [26]. Furthermore, the grain size in nugget zone for aluminum alloys is usually small and is distorted by the pin [27]. In addition, the shape of this zone may be changed due to the pin's figure. The nugget zone's profile in Fig. 5 is look more like to the taper followed by the tapered cylindrical shaped pin. Table 5 summarizes the results of metallographic tests and probable defects for samples of triangle and tapered

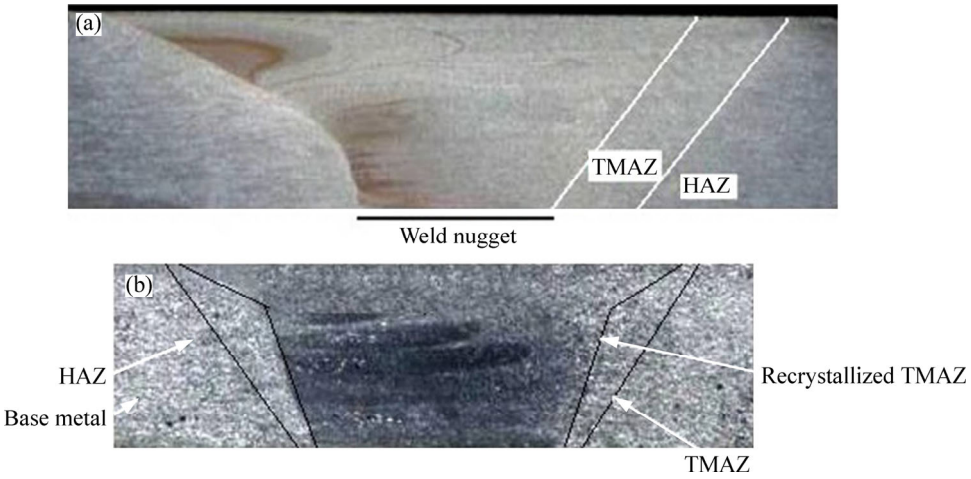

Fig. 5 Transects of friction stir welded samples [6]: (a) Three distinct zones, stirred (nugget) zone, thermo-mechanically affected zone (TMAZ) and heat-affected zone (HAZ); (b) Various micro structural zones

Table 5 Results of metallographic tests for samples which were welded using various profiles

Pin profile	Tool feature	Defect	Defect location	Macro-etch test
Tapered cylindrical	Threadless pin, flat shoulder	Tunnel in bottom of weld	Deficiency of heat transfer and incomplete melting	
Tapered cylindrical	Threadless pin, conical shoulder	No defect	—	
Tapered cylindrical	Threaded pin, conical shoulder	No defect	—	
Triangular	Threadless pin, flat shoulder	Tunnel in bottom of weld	Deficiency of heat transfer and incomplete melting	
Triangular	Threadless pin, conical shoulder	No defect	—	
Triangular	Threaded pin, conical shoulder	No defect	—	

cylindrical pins. In samples which were welded using flat shoulder and threadless pin, some defects were observed at the bottom of the weld, which was caused due to insufficient heat on the base metal. In other cases, no defect exists since the heat transfer was adequate and the metal flow was appropriate.

One of the mechanical properties which were studied in the current research was microhardness and it

was measured using Vickers microhardness method. Figures 6(a) and (b) represent the Vickers microhardness results for tapered cylindrical and triangle pin profiles. For all welded plates which were fabricated with six proposed tools, the hardness profiles have been become "W" shaped, which indicates a drop in the hardness value. In nugget zone, due to the recrystallization, the grains are situated coaxial and their sizes are become smaller, which result in a higher microhardness. In TMAZ, grains are stretched and deformed, which causes a sharp decrease in the hardness values. HAZ is located next to the TMAZ, and its structure looks like the base metal which means a graduate increase in the hardness.

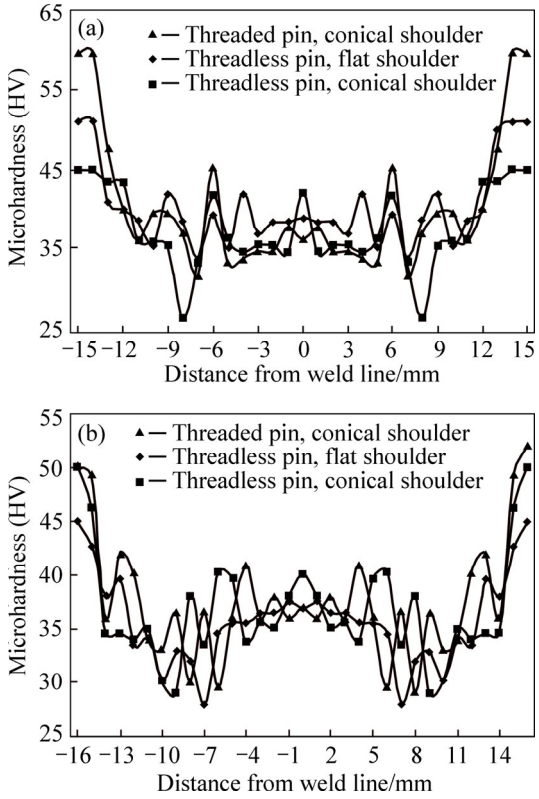

Fig. 6 Vickers microhardness test results for tapered cylindrical (a) and triangle pin (b) profiles

In tensile test, samples were fabricated according to ASTM-E08M tensile test standard and traverse speed during the process was adjusted at 3 mm/min. In order to compare the tensile results of welded sheets with base metal, an AA6061 plate was tested and the corresponding data is represented in Table 6. Besides, Table 7 summarizes the information related to tensile strength, yield strength, elongation, and the position where sample fractured. In all welded samples like the base metal, a ductile failure was observed but the positions of failure in samples were various. As can be seen in both profiles, tensile strength of weld zone enhanced in comparison with the base metal when pins were threaded and conical shoulders were utilized. The maximum value of elongation was observed when the welding process was done using threadless tapered cylindrical pin with flat shoulder. In other welded cases, the values of elongation were less than that of AA6061. Furthermore, except the sample which was welded using threadless triangular pin with flat shoulder, in other welded plates failure occurred in base metal. Threaded tapered cylindrical pin when the shoulder was conical resulted in the superior tensile strength. On the other hand, it is better to use flat shoulder threaded tapered cylindrical pin when elongation is the desired mechanical property.

For more illustration, yield strength, maximum tensile strength, and elongation comparisons for different pin profiles and base metal are given in Figs. 7−9.

A determinative criterion which was considered in specifying the structures of the models was MSE in validation step. Figures 10(a) and (b) illustrate the performance of the models and mean squared error values for two ANN models. MSE values for both networks were less than 10, which indicates appropriate trained models.

Figures 11 and 12 demonstrate the relationship between the experimental values and the answers of the ANNs for various steps of training procedure, and all

Table 6 Results of tensile test for base metal

Sample	Yield strength/MPa	Maximum tensile strength/MPa	Elongation/%	Failure feature
AA6061	22	140.5	15	Ductile failure

Table 7 Results of tensile test for welded samples using various pin profiles and different tools

No.	Pin profile	Tool feature	Yield strength/MPa	Maximum tensile strength/MPa	Elongation/%	Failure position
1	Triangular	Threadless pin, flat shoulder	25	122.8	5.2	Weld
2	Triangular	Threadless pin, conical shoulder	20	138.6	10	Base metal
3	Triangular	Threaded pin, conical shoulder	29	148.3	11	Base metal
4	Tapered cylindrical	Threadless pin, flat shoulder	20	143.3	16.3	Base metal
5	Tapered cylindrical	Threadless pin, conical shoulder	26	136.7	13.4	Base metal
6	Tapered cylindrical	Threaded pin, conical shoulder	33	145.4	11	Base metal

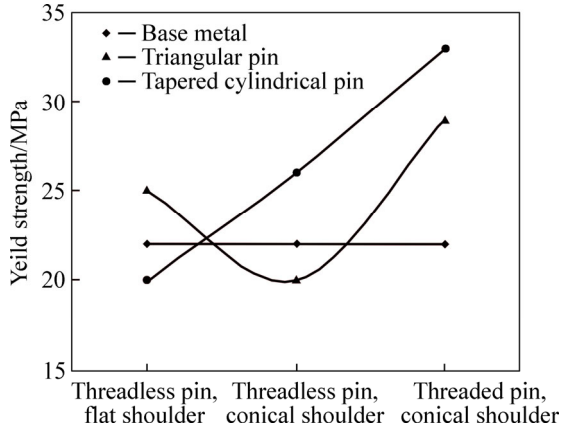

Fig. 7 Yield strength values for different pin profiles compared with base metal

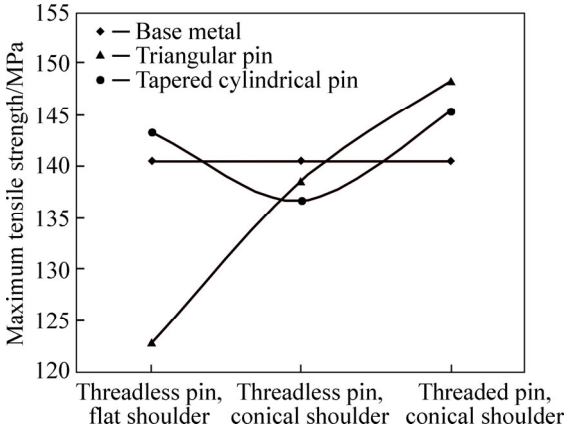

Fig. 8 Maximum tensile strength values for different pin profiles compared with base metal

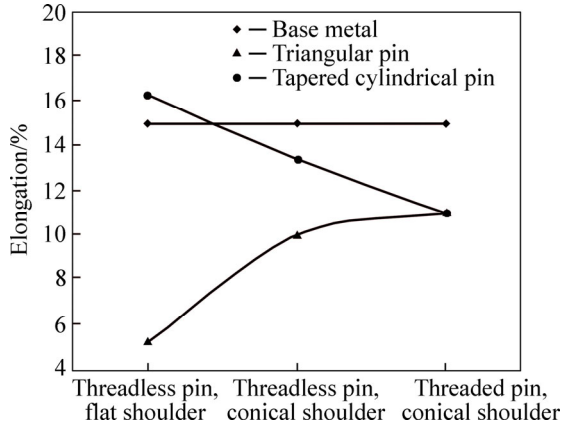

Fig. 9 Elongation values for different pin profiles compared with base metal

data were utilized in training procedure. The coefficient of determination indicates the convergence between experimental results and outputs of the model, and the more closer the amount to one, the more perfect the correlation between desired answers and predicted values. Therefore, coefficient of determination (R^2) between actual data and predicted answers was calculated to evaluate the performance of selected neural networks,

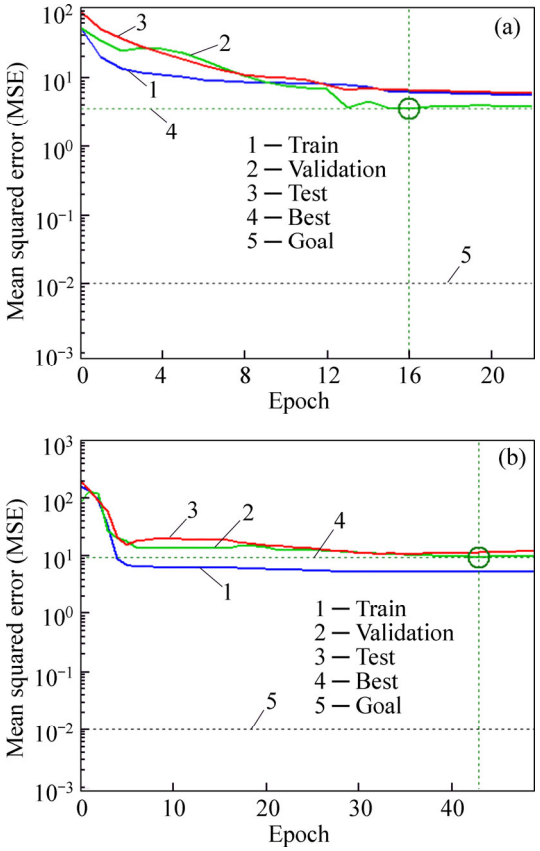

Fig. 10 MSE for ANN models for triangle pin profile (a) and tapered cylindrical pin profile (b) tools

and 0.8479 and 0.775 were assessed as values of R^2 which confirm the accuracy of designed models.

Mean absolute percentage error in training procedure and for test data sets was another criterion to evaluate the network's performance. The values of MAPE for all data were less than 5.56% and 4.55% for triangle and tapered cylindrical pin profile tools, respectively. Furthermore, MAPE values in test step for both models were less than 7.48%, which implies the reliable predictions of networks. Table 8 represents MAPE and MAE values in training procedure and test stage for both pin profiles.

4 Conclusions

1) AA6061 sheets were welded using triangle and tapered cylindrical shaped pin tools. Vickers microhardness test was performed in different distances from the weld line. The quality of the weld in concaved shoulders was better compared with the flat ones. Furthermore, in all welds, the microhardness in TMAZ has the least value while it experienced the maximum amount in the base metal.

2) Two feed forward back propagation artificial neural network techniques were employed to model and predict the Vickers microhardness of AA6061 friction

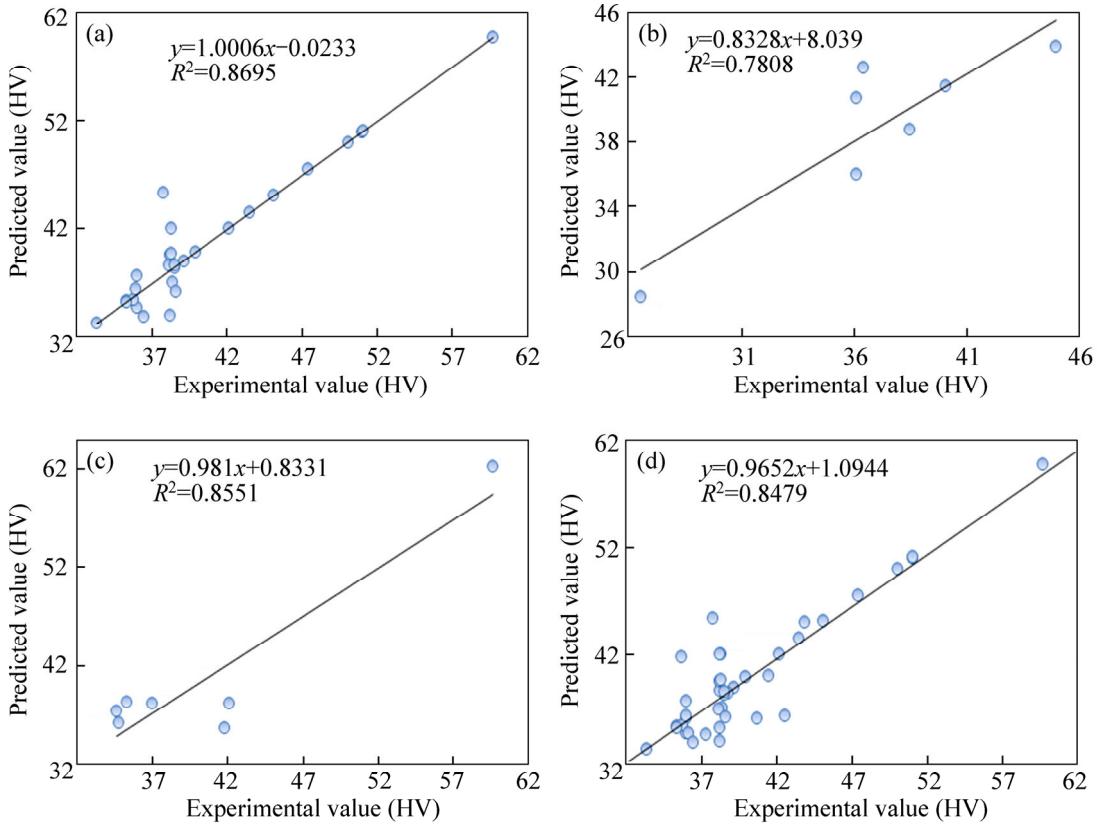

Fig. 11 Comparison of actual and predicted values of Vickers microhardness for tapered cylindrical pin profile in training (a), validation (b), test (c), and all data in training procedure (d)

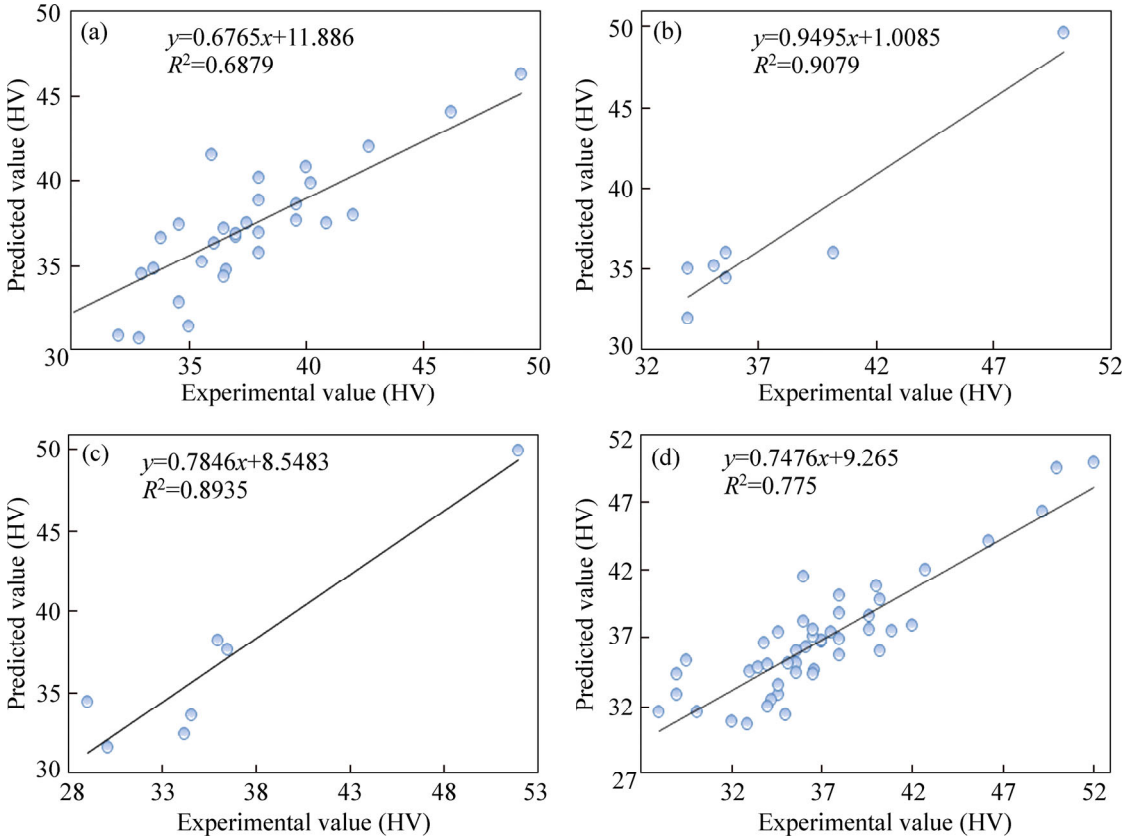

Fig. 12 Comparison of actual and predicted values of Vickers microhardness for triangle pin profile in training (a), validation (b), test (c), and all data in training procedure (d)

Table 8 MAPE and MAE for ANNs in this work

Pin profile	Network architecture	MAPE in training stage/%	MAE in training stage (HV)	MAPE for test sets/%	MAE for test sets (HV)
Triangular	3-8-1	5.398	1.9	7.48	2.62
Tapered cylindrical	3-7-3-1	4.41	1.67	6.024	2.068

stir welded plates. The values of MAPE in training process for both ANNs were less than 4.83%, which indicates that the answers of the models had acceptable deviance with actual values of microhardness.

3) Considering the acceptable results of the ANN models in this work, it can be concluded that this method can be utilized to model the mechanical procedures. Using mathematical modeling methods like ANN can save time, material and costs and results in optimized designs.

References

[1] NAGESWARA RAO P, JAYAGANTHAN R. Effects of warm rolling and ageing after cryogenic rolling on mechanical properties and microstructure of Al 6061 alloy [J]. Materials & Design, 2012, 39: 226−233.

[2] DAS H, CHAKRABORTY D, PAL T K. High-cycle fatigue behavior of friction stir butt welded 6061 aluminium alloy [J]. Transactions of Nonferrous Metals Society of China, 2014, 24(3): 648−656.

[3] RAJAKUMAR S, MURALIDHARAN C, BALASUBRAMANIAN V. Statistical analysis to predict grain size and hardness of the weld nugget of friction-stir-welded AA6061-T\n 6 aluminium alloy joints [J]. International Journal of Advanced Manufacturing Technology, 2011, 57(1/2/3/4): 151−165.

[4] PENG D, SHEN J, TANG Q, WU C, ZHOU Y. Effects of aging treatment and heat input on the microstructures and mechanical properties of TIG- welded 6061-T6 alloy joints [J]. International Journal of Minerals, Metallurgy, and Materials, 2013, 20(3): 259−265.

[5] OKUYUCU H, KURT A, ARCAKLIOGLU E. Artificial neural network application to the friction stir welding of aluminum plates [J]. Materials & Design, 2007, 28(1): 78−84.

[6] MISHRA R S, MA Z Y. Friction stir welding and processing [J]. Materials Science and Engineering R: Reports, 2005, 50(1/2): 1−78.

[7] ÇAM G, MISTIKOGLU S. Recent developments in friction stir welding of Al-alloys [J]. Journal of Materials Engineering and Performance, 2014, 23(6): 1936−1953.

[8] TOPIC I, HÖPPEL H W, GÖKEN M. Friction stir welding of accumulative roll-bonded commercial-purity aluminium AA1050 and aluminium alloy AA6016 [J]. Materials Science and Engineering: A, 2009, 503(1): 163−166.

[9] SUN Y, FUJII H, TAKADA Y, TSUJI N, NAKATA K, NOGI K. Effect of initial grain size on the joint properties of friction stir welded aluminum [J]. Materials Science and Engineering: A, 2009, 527(1): 317−321.

[10] UEMATSU Y, TOKAJI K, SHIBATA H, TOZAKI Y, OHMUNE T. Fatigue behaviour of friction stir welds without neither welding flash nor flaw in several aluminium alloys [J]. International Journal of Fatigue, 2009, 31(10): 1443−1453.

[11] LIU H J, ZHANG H J, YU L. Effect of welding speed on microstructures and mechanical properties of underwater friction stir welded 2219 aluminum alloy [J]. Materials & Design, 2011, 32(3): 1548−1553.

[12] BUFFA G, FRATINI L, MICARI F. Mechanical and microstructural properties prediction by artificial neural networks in FSW processes of dual phase titanium alloys [J]. Journal of Manufacturing Processes, The Society of Manufacturing Engineers, 2012, 14(3): 289−296.

[13] MISHRA R S, DE P S, KUMAR N. Friction stir processing [M]. New York: Springer, 2014.

[14] SHOJAEEFARD M H, BEHNAGH R A, AKBARI M, BESHARATI GIVI M K, FARHANI F. Modelling and Pareto optimization of mechanical properties of friction stir welded AA7075/AA5083 butt joints using neural network and particle swarm algorithm [J]. Materials & Design, 2013, 44: 190−198.

[15] SHOJAEEFARD M H, AKBARI M, ASADI P. Multi objective optimization of friction stir welding parameters using FEM and neural network [J]. International Journal of Precision Engineering and Manufacturing, 2014, 15(11): 2351−2356.

[16] GHETIYA N D, PATEL K M. Prediction of tensile strength in friction stir welded aluminium alloy using artificial neural network [J]. Procedia Technology, 2014, 14: 274−281.

[17] PALANIVEL R, MATHEWS P K. Prediction and optimization of process parameter of friction stir welded AA5083-H111 aluminum alloy using response surface methodology [J]. Journal of Central South university, 2012, 19(1): 1−8.

[18] MOOSABEIKI V, AZIMI G, GHAYOOR M. Influences of tool pin profile and tool shoulder curvature on the formation of friction stir welding zone in AA6061 aluminum alloy [J]. Advanced Materials Research, 2012, 445: 789−794.

[19] RAFIQ M, BUGMANN G, EASTERBROOK D. Neural network design for engineering applications [J]. Computers & Structures, 2001, 79(17): 1541−1552.

[20] HAYKIN S S. Neural networks and learning machines [M]. Pearson Education Upper Saddle River, 2009: 3.

[21] COLEGROVE P, SHERCLIFF H R. 3-dimensional CFD modelling of flow round a threaded friction stir welding tool profile [J]. Journal of Materials Processing Technology, 2005, 169(2): 320−327.

[22] CHOWDHURY S M, CHEN D L, BHOLE S D, CAO X. Tensile properties of a friction stir welded magnesium alloy: Effect of pin tool thread orientation and weld pitch [J]. Materials Science and Engineering A, 2010, 527(21/22): 6064−6075.

[23] VENKATESHA B N, BHAGYASHEKAR M S. Preliminary studies on mecahnical and metallurgical behaviour of friction stir welded butt joints [J]. Procedia Engineering, 2014, 97: 847−853.

[24] LIENERT T J, STELLWAG JR W L, GRIMMETT B B, WARKE R W. Friction stir welding studies on mild steel [J]. WELDING JOURNAL-NEW YORK-, 2003, 82(1): 1−S.

[25] SUTTON M A, REYNOLDS A P, YANG B, TAYLOR R. Mixed mode I/II fracture of 2024-T3 friction stir welds [J]. Engineering Fracture Mechanics, 2003, 70(15): 2215−2234.

[26] LOHWASSER D, CHEN Z. Friction stir welding: From basics to applications [M]. Elsevier, 2009.

[27] MILES M P, NELSON T W, STEEL R, OLSEN E, GALLAGHER M. Effect of friction stir welding conditions on properties and microstructures of high strength automotive steel [J]. Science and Technology of Welding & Joining, 2009, 14(3): 228−232.

(Edited by YANG Hua)